Chemosphere 287 (2022) 132143

Contents lists available at ScienceDirect

Chemosphere

journal homepage: www.elsevier.com/locate/chemosphere

Development, validation, and application of a new method for the quantitative determination of monohydrogen-substituted perfluoroalkyl carboxylic acids (H–PFCAs) in surface water

Mo Awchi [a], Wouter A. Gebbink [b], Bjorn J.A. Berendsen [a], Jonathan P. Benskin [c], Stefan P. J. van Leeuwen [a,*]

[a] Wageningen Food Safety Research, Wageningen University & Research, Akkermaalsbos 2, 6708, WB, Wageningen, the Netherlands
[b] PFA-Brussels Sprl, 1040, Brussels, Belgium
[c] Department of Environmental Science, Stockholm University, Stockholm, Sweden

HIGHLIGHTS

- Hydrogen-substituted perfluoroalkyl carboxylic acids (H–PFCAs) are PFAS alternatives emerging in the environment.
- An WCX-SPE-LC-MS/MS method was developed, optimized, and validated, using an ion-pairing agent.
- Quantification; After application on surface water, H–PFCAs were found in trace levels and PFCAs in high concentration.

ARTICLE INFO

Handling editor: Jerzy Falandysz

Keywords:
PFAS
PFCAs
H–PFCAs
LC-MS/MS
Surface water

ABSTRACT

Per- and polyfluoroalkyl substances (PFASs) are a large and diverse class of chemicals. While some have been phased out internationally due to concerns over their human and environmental health risks, novel alternative PFASs continue to be manufactured and detected in environmental samples. The occurrence and fate of these alternatives remain poorly understood. The present study investigated the occurrence of an emerging class of PFAS alternative, the monohydrogen-substituted perfluoroalkyl carboxylic acids (H–PFCAs), in conjunction with the more well-known PFCAs. A weak anion exchange solid phase extraction-liquid chromatography tandem mass spectrometry method for quantitative determination of H–PFCAs in surface water was developed, validated, and applied on samples collected from the Netherlands. To improve chromatography, especially for short-chain (H-) PFCAs, an ion-pairing agent, tetrabutylammonium hydrogen sulphate, was used. The method was validated for linearity ($R^2 > 0.99$), instrumental detection limits (0.01–0.09 ng/mL), method detection limits (0.03–0.75 ng/mL), matrix effects (<20%), percent absolute- and relative recovery (57–121%), trueness (130-80%), repeatability (<20%), and within-lab reproducibility (<20%). Eleven out of fourteen PFASs showed acceptable results. Application of the newly validated method to surface water throughout the Netherlands revealed trace levels of H–PFCAs (including two new H–PFCAs) and high concentrations of PFCAs.

1. Introduction

Per- and polyfluoroalkyl substances (PFASs) are mostly anthropogenic chemicals that have been manufactured since the 1940s. The unique stain and water-repellent properties of highly fluorinated aliphatic chains have led to the widespread use of PFASs in consumer products, for example as surfactants and surface protectors in a variety of applications including textiles and food contact paper and packaging. Their surface tension-lowering properties, along with thermal and chemical stability have also led to applications in firefighting foams (AFFF), fluoropolymer manufacturing, hydraulic fluids, and a range of other applications (Glüge et al., 2020).

The number of identified PFASs on the global market has rapidly increased over the last few decades. The OECD PFAS database currently lists 4730 substances (OECD, 2021) and the historical global production of PFASs was estimated at several hundred thousand metric tons

* Corresponding author.
E-mail address: Stefan.vanLeeuwen@wur.nl (S.P.J. van Leeuwen).

https://doi.org/10.1016/j.chemosphere.2021.132143
Received 27 June 2021; Received in revised form 26 August 2021; Accepted 31 August 2021
Available online 3 September 2021

annually (Buck et al., 2011). The wide use and application of PFASs have led to the occurrence of these compounds in the global environment including wildlife and human blood samples (Xiao, 2017). Long-chain perfluoroalkyl carboxylic acids (PFCAs; i.e. ≥ eight carbon atoms) are among the most commonly observed PFASs in the environment. In addition to their persistence and bioaccumulation potentials, exposure to PFCAs has been linked to tumor growth and immunotoxicity (EFSA et al., 2020) (DeWitt, 2015). Due to the health risks associated with these substances, phase-out of perfluorooctane sulfonate (PFOS), long-chain PFCAs such as perfluorooctanoic acid (PFOA), and related chemicals was initiated by their major manufacturing companies and the United States Environmental Protection Agency (EPA, 2000) (P.O.P. R., 2015). In addition, PFOS, PFOA, their precursors, and other PFASs are listed under the Stockholm Convention on Persistent Organic Chemicals and are regulated in the EU chemicals legislation (Swedish Chemicals Agency, 2021).

As a consequence of increased regulation of long-chain PFASs, industry has shifted its production to shorter-chain length and replacement chemistries, such as perfluoro-2-hydroxypropanoic acid (HFPO-DA) a perfluoro ether carboxylic acid (Gebbink et al., 2017). These shorter chain PFASs and alternatives are intended to be less bioaccumulative and toxic than long-chain PFASs. However, recent studies showed that some PFAS alternatives and short chain PFAS display considerable persistence and may impart equal or stronger adverse effects than legacy PFASs (Krippner et al., 2015) (Sheng et al., 2018) (Gaballah et al., 2020) (Li et al., 2020a). Therefore, there is an urgent need to identify and quantify replacements to long-chain PFASs.

Commonly reported alternatives to long-chain PFASs which have been measured in surface water include polyfluoroalkyl ether carboxylic acids (PFECAs; e.g. HFPO-DA) and 3H-perfluoro-3-[(3-methoxy-propoxy)propanoic acid] (ADONA) (Fromme et al., 2017) (Zhang et al., 2019) (Gebbink et al., 2017). However, non-targeted screening approaches (Hensema et al., 2021) have identified several other novel PFASs such as monohydrogen substituted PFCAs (H–PFCAs), polyhydrogen-substituted PFCAs, monochlorine substituted PFCAs, monoether PFECAs, and polyether PFECAs in surface waters, sediment, sludge, biota, and human blood (Barrett et al., 2021) (Song et al., 2018) (Liu et al., 2015) (Washington et al., 2015) (Newton et al., 2017). The occurrence of these alternatives could originate from sources such as industrial and/or consumer uses (Buck et al., 2011) (Wang et al., 2018) (Gebbink et al., 2017); however, as opposed to the major long-chain PFAS, the magnitude of emissions and the environmental fate of these emerging PFASs remain poorly understood.

Most studies on newly identified PFAS alternatives are qualitative, involving suspect and non-targeted approaches. Quantitative methods for alternatives are sparse, especially when analytical standards are unavailable for method development. Specifically, studies involving detection of H–PFCAs in surface water, sediment (Liu et al., 2015) (Song et al., 2018), human blood (Li et al., 2020b), and biota (Barrett et al., 2021) only mention the (tentative) identification and area count of these compounds. While Barrett et al. (2021) showed an increasing temporal trend of short-chain PFCAs and H–PFCAs in Beluga whales, the magnitude of emission of these compounds remains poorly understood.

This study aims to take a first step towards accurate quantification of C4–C11 (H-)PFCAs. A targeted liquid chromatography – triple quadrupole mass spectrometric (LC-MS/MS) method for quantitative analysis of H–PFCAs, in conjunction with well-known PFCAs was developed. Chromatographic and MS parameters were optimized, and the method was validated by determining the linearity, method limit of detection (M-LOD) and method limit of quantification (M-LOQ), instrument LOD (I-LOD), instrument LOQ (I-LOQ), matrix effects, absolute- and relative recovery, trueness, repeatability, and within-lab reproducibility (EU, 2002). The method was applied to surface water samples from the Netherlands to provide insight into the environmental occurrence of PFCAs and H–PFCAs.

2. Experimental

2.1. Chemicals and standards

Water was deionized and passed through a Milli-Q water purification system (Millipore, Billerica, MA, USA). Acetonitrile (UPLC-MS grade) and methanol (UPLC-MS grade) were purchased from Actu-All (Oss, the Netherlands). Ammonium hydroxide (25%) was purchased from VWR International (Amsterdam, the Netherlands). Ammonium solution (25%) and sodium acetate trihydrate were obtained from Merck (Darmstadt, Germany). Sodium hydroxide, ammonium acetate 98%, and tetrabutylammonium hydrogensulfate (TBAS) were purchased from Sigma (St. Louis, USA). Perfluoropentanoic acid (PFPA), perfluorohexanoic acid (PFHxA), perfluoroheptanoic acid (PFHpA), perfluorooctanoic acid (PFOA), perfluorononanoic acid (PFNA), perfluorodecanoic acid (PFDA), perfluoroundecanoic acid (PFUnDA), perfluorododecanoic acid (PFDoDA), acid were purchased from Wellington Laboratories (Guelph, Canada) as a mixture of 2 μg/mL $^{13}C_2$-perfluoroheptanoic acid, $^{13}C_4$-perfluorooctanoic acid, $^{13}C_5$- perfluorononanoic acid, $^{13}C_2$-perfluorodecanoic acid, $^{13}C_2$-perfluoroundecanoic acid, $^{13}C_2$- perfluorododecanoic acid were obtained from Wellington Laboratories as a 2 μg/mL mixture in MeOH. 4-hydrogen-polyfluorobutanoic acid (H-PFBA), 5-hydrogen-polyfluoropentanoic acid (H-PFPA), 7-hydrogen-polyfluoroheptanoic acid (H-PFHpA), 8-hydrogen-polyfluorooctanoic acid (H-PFOA), 9-hydrogen-polyfluorononaoic acid (H-PFNA) and 11-hydrogen-polyfluoroundecanoic acid (H-PFUnDA) from Apollo scientific (Manchester, United Kingdom). Further details on PFCAs and H–PFCAs, including CAS numbers, are presented in Supporting Information Table S1.

2.2. Preparation of extracts

Surface water samples were collected from several locations in the Netherlands on June 26th, 2019. The samples were taken from diverse water bodies, including industrial areas, areas close to a fluorochemical plant (Gebbink et al., 2017), and ponds with no clear linkage to any fluorochemical plant/industrial areas (see Fig. 1 and Table S2). Samples

Fig. 1. Water sampling locations throughout the Netherlands. See Table S2 for more information on the sampling locations.

were taken by filling High-Density Polyethylene (HDPE) wide-mouth bottles (1000 mL; VWR, Radnor, USA) using a metal bucket. On the sampling day, 2 sealed HDPE bottles with 1 litre of Milli-Q water were brought along during sampling to serve as field blanks. After each collection, the bucket was rinsed with the river water from the new location before sampling to prevent cross-contamination between consecutive samples. After sampling, the samples were stored at 4 °C prior to extraction. For method validation, local tap- and river water collected near Wageningen, the Netherlands (sampling location R10) was used.

The sample preparation procedure for PFCAs was adapted from Gebbink et al. (2017). In short, 200 mL of water was spiked with a 25 μL internal standard mix (see SI section Sample Extraction). Thereafter, an Oasis WAX cartridge (6 cc, 150 mg, 30 μm; Waters Milford, USA) was conditioned with 8 mL of methanol and 8 mL Milli-Q. The sample was loaded on the cartridge and subsequently washed with 5 mL 25 mM sodium acetate buffer and 3 mL methanol. Elution of the analytes from the SPE column was achieved with 2% ammonia in acetonitrile. The eluent was evaporated until dryness under a gentle stream of nitrogen at 40 °C using a Turbovap LV (Caliper Life Sciences, Waltham, USA). The residue was dissolved in 575 μL of acetonitrile, 25 μL of a$^{13}C_8$-PFOA recovery standard (100 ng/mL) was added, and the extract was sonicated for 5 min. After sonication, 400 μL of 62.5 mM of TBAS in Milli-Q was added and the extract was sonicated again for 5 min. Hereafter, the supernatant was transferred to a filter vial (Filter vials 0.45 μm pore size; (Whatman Mini-UniPrep, PTFE, Buckinghamshire, USA)) and was ready for injection.

2.3. Instrumental analysis

The UHPLC-MS/MS system consisted of a Shimadzu LC system (Shimadzu Corporation, Kyoto, Japan) connected to a Sciex QTrap 5500 (Sciex, Framingham, MA, USA). An Acquity UPLC BEH C18 analytical column (50 mm × 2.1 mm i.d., 1.7 μm, Waters) was used for chromatographic separation and was running at 35 °C. The mobile phase consisted of 2 mM ammonium acetate in water (A) and acetonitrile (B). The gradient elution program started with 25% B and was held for 3 min, followed by a linear gradient to 100%B in 2.5 min. The 100% B was held for 2.5 min before returning to the initial mobile phase ratio at 1 min and was held for 3.5 min. The total run-time was 12.5 min with a flow rate of 0.3 mL/min. The injection volume was 20 μL. A Symmetry C18 analytical column (50 mm × 2.1 mm i.d., 5 μm, Waters, MA, USA) was placed upstream from the injector to delay any potential contamination from fluoropolymer components in the LC system and sample injection.

For the MS detection, nitrogen was used as the nebulizing and drying gas. The triple quadrupole was operated using an electrospray ionization (ESI) interface in negative mode with an ion spray voltage of −4500 V, a curtain gas flow of 30 L/h, the temperature at 350 °C, and the collision gas were set at high. For the instrumental analysis, a calibration curve was prepared ranging from 0.05 to 25 ng/mL. A full overview of calibration curve dilutions is shown in Table S3.

2.4. Method development and validation

A method described by Gebbink et al. (2017), was used as a starting point for chromatographic method development. A 5 ng/mL standard solution together with different mobile phase compositions and ion-pairing agent concentrations were used to optimize chromatographic resolution, retention, and total run-time. After satisfactory chromatography and retention, the method for analysis of river water was validated in a 3-day experimental setup. The analytical quality control and method validation document, N SANTE/12682/2019 (EURL, 2019), was used as starting point for the validation. On three separate occasions, 200 mL of tap water was fortified to three concentrations (1 ng/L, 5 ng/L, and 25 ng/L). Five replicates, at each of the three spiking levels, were analyzed on each day. Linearity, method limit of detection (M-LOD), method limit of quantification (M-LOQ), instrumental limit of detection (I-LOD), and instrumental limit of quantification (I-LOQ), matrix effects, absolute- and relative recovery, trueness, repeatability, and within-lab reproducibility were determined (see Equations S1–S7 for calculations). For quantification of PFCAs, exactly matched isotopically labeled internal standards were used (Table S1). For H–PFCAs, ^{13}C–PFCAs of a corresponding chain length were used as internal standards (e.g. 8H-PFOA was quantified using ^{13}C-PFOA). As all river-water samples contained trace levels of both H–PFCAs and PFCAs, a local river-water sample (R10), was collected and spiked at 30 ng/L (6- and 4- fold above background levels in river-water for H–PFCAs, and PFCAs respectively). Thereafter, matrix effects, absolute- (non-internal standard corrected) and relative (internal standard corrected) recovery, trueness, reproducibility, and within-lab reproducibility were determined.

3. Results and discussion

3.1. LC-ESI-MS/MS method development

3.1.1. Liquid chromatography optimization

Using PFCA and H-PFCA analytical standards, the method was optimized in terms of chromatographic separation, chromatographic peak shape, and total run time. Initial chromatographic separation was performed on an Acquity UPLC BEH column in combination with a water-acetonitrile mobile phase. This led to early chromatographic elution and insufficient separation for shorter chain PFASs, perhaps in part due to the composition of the loading solvent, especially for C4, C5, and C6 (H-)PFCAs. To improve the chromatography of the shorter chain-length PFAS, ion-pairing reagents such as TBAS can be added to the sample vial (Esparza et al., 2011). TBAS was added to a 5 ng/mL (H-)PFCA solution while the mobile phases, gradient, and all other conditions were maintained as described in section 2.4. The presence of TBAS improved the overall peak shape and retention of the shorter chain length PFAS on the LC-column, as shown in the Total Ion Current (TIC) chromatograms (Fig. 2). The total gradient run-time with the addition of TBAS remained the same.

3.1.2. Tandem mass spectrometry optimization

For each analyte, two different MS transitions (i.e. qualifier, and quantifier ion) were optimized (Table S3). Using 10 ng/mL analytical standards, MS/MS settings including declustering potential (DP), entrance potential (EP), collision energy (CE), and collision cell exit potential (CXP) were optimized by continuous direct infusion of standards. Thereafter, the effect of TBAS on the signal intensity of (H-)PFCAs was investigated. TBAS was added at 3 different concentrations (12.5, 25, and 50 mM) to a 2 ng/mL solution containing (H-)PFCAs while the mobile phase and all other conditions were kept as described in section 2.4. Little to no difference was observed between 12.5 and 25 mM TBAS and a slight drop in signal intensity for 50 mM (Figure S1). 25 mM was chosen as the preferred concentration due to higher expected matrix content for river-water samples, leaving a buffer in case a majority of TBAS binds to the matrix.

Figure S2 shows the signal intensity of a 10 ng/mL standard injection for all (H-)PFCAs with the method described by Gebbink et al. (2017), (method 1, without TBAS) and the same method but with the addition of 25 mM TBAS as an ion-pairing agent added to the LC-vial (method 2) (n = 3). As can be seen in Figure S2, method 2 performs worse in terms of signal intensity in comparison to method 1 due to the addition of TBAS, especially for the shorter chain-length (H-)PFCAs. To solve this sensitivity drop, the MS settings were tuned for all analytes, in particular the DP and EP with the addition of TBAS. Table S4 shows optimized MS/MS parameters. Despite this effort, the signal remained higher for method 1. However, the addition of TBAS improved the overall signal-to-noise ratio (Fig. 2), leading to improved LOQs. In addition, the improved

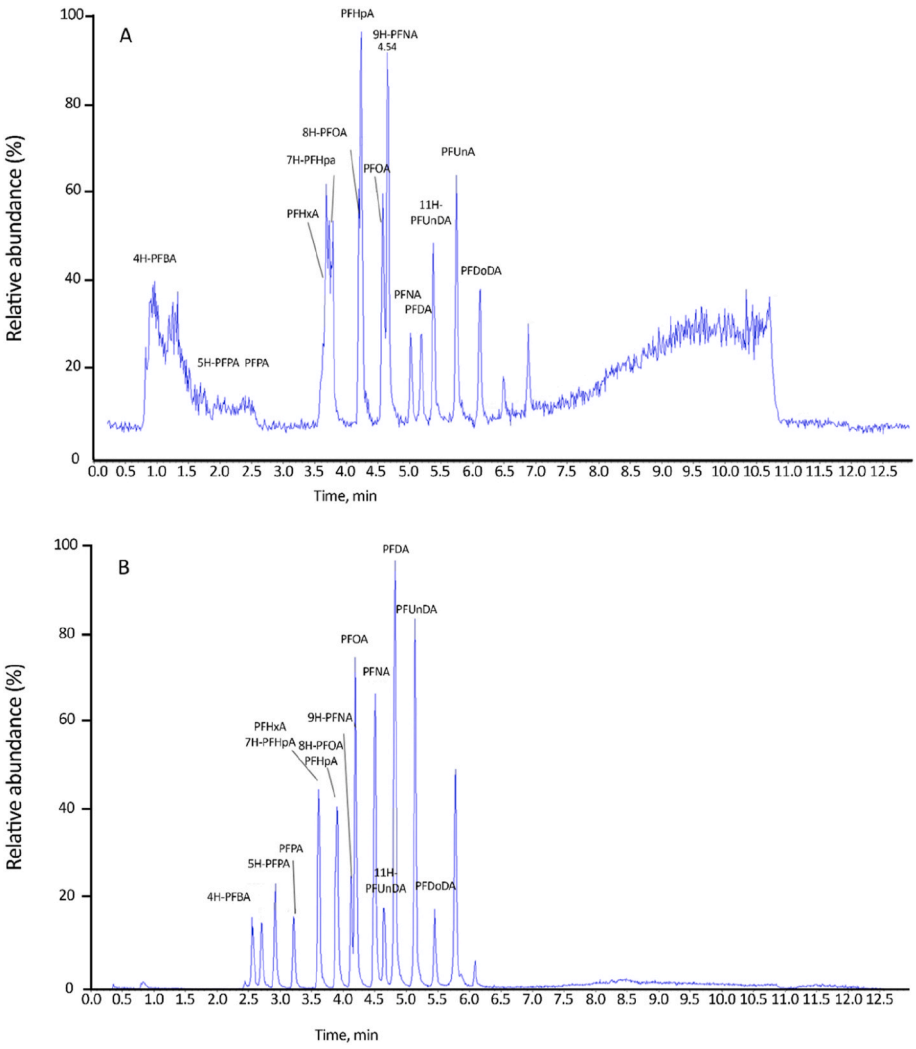

Fig. 2. Chromatographic separation of a standard solution of (H-)PFCAs (5 ng/mL) in the method without TBAS (A) and with the addition of 25 mM TBAS as an ion-pairing agent (B) on an Acquity UPLC BEH C18 column.

peak shapes with the use of TBAS resulted in a more refined peak integration due to the gaussian nature of the peaks (Fig. 2B). Therefore, method 2 was chosen as the preferred method.

3.1.2.1. Tandem mass spectrometry setting and fragmentation prediction. Due to the lack of commercially available standards for 6H-PFHxA, 10H-PFDA, the MS settings and transitions for these analytes could not be optimized experimentally. To overcome this, MS transitions were predicted from the observed fragmentation pattern of the neighboring analytes. For example, the 10H-PFDA settings were deduced from 11H-

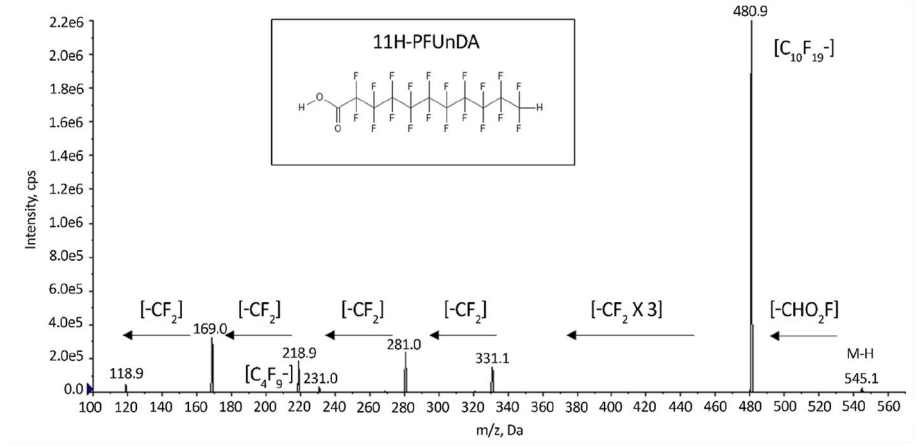

Fig. 3. Fragmentation pattern of 11H-PFUnDA.

PFUnDA (Fig. 3), assuming a similar fragmentation behaviour while CE settings for 10H-PFDA were predicted by taking the average CE values of its chain-length neighbors (i.e. 9H-PFNA and 11H-PFUnDA). All H–PFCAs have their most intense fragment at molecular ion peak (M) minus 64 Da which corresponds to a neutral loss of HF and CO_2. Therefore, the transition for the missing H–PFCAs was set at to $[M-64]^-$ as well. Table S4 shows all the transitions, including those predicted for the missing H–PFCAs. After initial CHO_2F loss, both PFCAs and H–PFCAs lose CF_2 consecutively from their chain as shown in Fig. 3. While the exact location of the hydrogen substituent in H-PFCA standards could not be confirmed by the supplier (or via our fragmentation experiments), the fragmentation pattern observed here is similar to that reported previously for purported terminal H–PFCAs (Song et al., 2018) (Liu et al., 2015) (Liu et al., 2018). Nevertheless, future work should confirm the position of the H-substituent, for example using ^{1}H NMR.

3.1.3. Instrumental performance & quantification

Quantification was performed by using isotopically labeled PFCA standards (Table S1) and calculating relative response factors (RRFs) using Equation S1. For quantification of H–PFCAs, the internal standard of the equivalent chain-length PFCA equivalent was used. For the missing H–PFCAs, RRFs were predicted based on the average value of the chain-length neighbors. I-LOD and I-LOQ values were determined by injecting a 0.5 ng/mL solution (equivalent to 50 pg on column) containing all analytes and thereafter determining the concentration corresponding to a signal-to-noise ratio of 3- and 10, respectively (Table 1). Confirmation of the calculated I-LOD/LOQ was achieved by injecting standards near the I-LOD/LOQ concentration and re-calculating these parameters as described above. Linearity (0.005–25 ng/mL) was calculated by applying least squares regression on the calibration curve (Table S4) which was corrected with the use of internal standards. Table 1 shows instrumental performance parameters and RRF values for quantification (n = 1). All analytes displayed excellent linearity (R^2 > 0.99).

3.2. Method validation

3.2.1. Method LOD/LOQ, recovery, and matrix effect

The aforementioned approach to determine I-LOD and I-LOQ was applied to determine M-LOD and M-LOQ. However, this time tap water samples were spiked around 0.5 ng/mL (i.e. the targeted concentration in the final extract after sample preparation) and were injected into the LC-MS/MS system. The absolute- and relative recovery was calculated according to Equation S2. Matrix-induced ionization effects were determined in two ways for the tap water matrix. First, matrix effects (ME) were determined by comparing the differences in IS-corrected signal intensities between spiked tap water samples to a concentration equivalent standard solution using Equation S3 (8 spike levels, n = 1). Second, relative matrix effects (RME) were estimated by comparing the slopes of a calibration curve prepared using tap water (normalized using an internal standard) to the slope of the corresponding calibration curve in solvent (normalized using an internal standard using Equation S4). Regarding M-LOD and M-LOQ, the values for all analytes are comparable except for PFPA and PFHxA which were higher compared to the other (H-)PFCAs, which is in line with the observation for I-LOD and I-LOQ. Previously reported M-LOQ for PFASs spiked in Milli-Q water was similar to the present work (Gebbink et al., 2017). Absolute- and relative recoveries of the (H-)PFCAs ranged between 57 and 121%; lower percent absolute recoveries observed for chain lengths >C10 could be a consequence of adsorption by the filter vial used in the last step of sample clean-up (Berendsen et al., 2020). Except for >C10 PFCAs and PFPA (121%), all (H-)PFCAs were within the set 70–120% criteria for absolute recovery (EURL, 2019). ME and RME were <20% for all compounds, except PFDoDA, and were considered acceptable (see Table 2 for results).

3.2.2. Trueness, repeatability, and within-lab reproducibility

For all fourteen compounds, trueness, repeatability, and within-lab reproducibility were determined using tap water fortified at 1, 10, and 25 ng/L and river-water (sample R10) fortified to 30 ng/L. The higher spiking level of 30 ng/L for the river water was necessary due to the higher level of background (H-)PFCAs in this matrix. The method was validated in a 3-day experimental setup (Section 2.5). Grubbs' outlier test was performed for the removal of abnormal values. Table 3 provides trueness, repeatability, and within-lab reproducibility results. All trueness results were in line with the set criteria of 70–130% except 4H-PFBA and PFPA at 1 ng/L spike levels. For repeatability, all compounds agreed with the set criteria of <20%, except PFPA at 10 ng/L. For within-lab reproducibility, all compounds, except 4H-PFBA, PFPA, and 5H-PFPA at 30 ng/L (river water), 10 ng/L, and 30 ng/L (river water), were within the set 20% variation limit (EURL, 2019).

Table 1
Summary of instrument limit of detection and quantification (I-LOD, I-LOQ), linearity and relative response factor (RRF) for standards.

Compound	I-LOD (ng/mL)	I-LOQ (ng/mL)	Linearity R^2	RRF[b]
PFPA	0.09	0.30	0.999	0.8
PFHxA	0.07	0.23	0.999	0.9
PFHpA	0.02	0.07	0.999	1.1
PFOA	0.01	0.03	0.996	0.9
PFNA	0.01	0.03	0.997	0.9
PFDA	0.02	0.07	0.996	0.9
PFUnDA	0.08	0.27	0.996	1.0
PFDoA	0.03	0.10	0.999	0.9
4H-PFBA	0.02	0.07	0.999	1.5
5H-PFPA	0.04	0.13	0.997	1.7
6H-PFHxA[a]				1.4
7H-PFHpA	0.04	0.13	0.997	1.1
8H-PFOA	0.02	0.07	0.999	0.3
9H-PFNA	0.04	0.13	0.999	0.4
10H-PFDA[a]				0.3
11H-PFUnDA	0.03	0.10	0.999	0.2

[a] Predicted values.
[b] RRF calculated at 5 ng/mL.

Table 2
Summary of method detection and quantification limits (MDL and MQL, respectively), relative matrix effects (i.e. internal standard corrected; RME), matrix effects (i.e. absolute/non-internal standard corrected; ME), and percent absolute- and relative recovery obtained for tap water.

Compound	Tap Water Matrix					
	MDL (ng/L)	MQL (ng/L)	Absolute Recovery (%)	Relative recovery (%)	ME (%)[a]	RME (%)[a]
PFPA	0.75	2.5	75	121	−35	−7.0
PFHxA	0.1	0.33	84	97	−14	1.2
PFHpA	0.03	0.10	78	100	−2.5	−0.3
PFOA	0.06	0.20	82	92	−17	−3.4
PFNA	0.02	0.07	84	92	−0.8	−0.8
PFDA	0.04	0.13	76	86	−3	−0.5
PFUnDA	0.10	0.33	65	80	−16	0.4
PFDoDA	0.04	0.13	57	87	−28	2.0
4H-PFBA	0.04	0.13	86	114	−23	14
5H-PFPA	0.05	0.17	96	117	−1.5	−5.6
7H-PFHpA	0.10	0.33	88	114	−30	1.5
8H-PFOA	0.10	0.33	94	105	−1.0	−11.7
9H-PFNA	0.03	0.10	87	97	−11	3.5
11H-PFUnDA	0.10	0.33	91	113	−12	−19.7

[a] Values for ME represent ion suppression (ME<0%), or ion enhancement (ME>0%), whereas RME represent the effect of the matrix on the sensitivity of the method (RME<0%, percent loss of sensitivity, RME>0%, percent gain in sensitivity.

Table 3
Trueness, repeatability, and within-lab reproducibility for (H-)PFCAs at 1, 10, 25 ng/L for tap water and 30 ng/L for river water.

		4H-PFBA	PFPA	5H-PFPA	PFHxA	PFHpA	7H-PFHpA	PFOA	8H-PFOA	PFNA	9H-PFNA	PFDA	PFUnDA	11H-PFUnDA	PFDoDA
Trueness (%)	**1**	131.0	136.7	120.6	109.4	100.7	116.5	105.9	100.5	100.1	101.4	96.3	88.3	106.7	98.1
	10	110.4	105.9	108.9	126.3	101.3	110.4	106.9	105.4	106.9	105.5	105.5	110.2	124.5	109.5
	25	82.7	108.3	109.5	97.6	105.6	101.9	102.6	97.2	102.4	94.9	97.0	110.20	111.3	101.8
	30[a]	89.3	82.8	66.4	99.2	94.0	88.8	104.0	102.5	102.4	129.2	96.6	106.8	106.3	112.3
Repeatability (%)	**1**	7.9	15.9	6.5	4.0	3.9	6.3	4.6	5.8	6.8	4.6	5.3	5.6	8.3	7.3
	10	6.1	37.5	5.3	3.5	7.1	5.4	3.5	4.0	6.2	4.3	3.7	5.3	15.1	6.9
	25	6.6	13.3	6.7	5.4	3.8	5.1	4.4	6.9	4.6	4.1	4.3	4.6	6.8	5.3
	30[a]	3.5	9.3	3.3	4.3	4.3	3.9	2.5	3.2	3.7	3.0	2.7	3.3	3.8	3.2
Within-lab reproducibility (%)	**1**	13.6	27.5	11.3	6.9	6.8	10.9	8.0	10.0	11.8	8.0	9.2	9.8	14.3	12.7
	10	10.7	64.9	9.2	6.1	12.4	9.4	6.0	6.9	10.8	7.5	6.3	9.2	26.2	12.0
	25	11.4	23.0	11.6	9.3	6.6	8.8	7.6	11.9	8.0	7.1	7.4	8.1	11.8	9.2
	30[a]	27.5	28.7	45.9	6.5	6.6	10.2	7.3	8.2	5.1	6.0	8.2	9.9	6.4	13.2

[a] Performed in river water.

3.3. Method application

The validated method was applied to surface water samples collected in the Netherlands.

3.3.1. Quality of the data

To assure the quality of the data, two field blanks, and three method blanks were analyzed (200 mL of Milli-Q spiked with isotopically labeled internal standards). Concentrations in surface water samples were only considered if the concentrations exceeded 3 times the concentration found in the method or field blank. To avoid false positives which may occur from co-elution of H–PFCAs isomers with the H–PFCAs of interest in the present work, retention time, identifier- and quantifier fragments, and ion ratios (allowed deviation of ±20%) were confirmed for all targets. Concentrations were determined with internal standard corrected values using an in-solvent calibration curve.

3.3.2. Application to field river-water samples

Concentrations of detected PFCAs and H–PFCAs are shown in Table 4. All PFCAs mentioned in this study were detected in all samples with ∑PFCA concentrations ranging between 29.9 and 121.6 ng/L. Additionally, for the H–PFCAs, 4H-PFBA was detected in all the samples with concentrations ranging between 1.4 and 2.0 ng/L 5H-PFPA and 7H-PFHpA were detected less frequently and at lower concentrations (<0.6 ng/L). The highest sum (H-)PFCA concentration was found in sample R2, which was sampled just downstream from a fluorochemical plant, and is in line with observations by Gebbink et al. (2017). PFPA, PFHxA, PFHpA, and PFNA are roughly 2 times higher and PFOA and PFDA are roughly 3 times higher than previously reported (Gebbink et al., 2017).

To the best of our knowledge, this is the first time that 4H-PFBA and 5H-PFPA have been detected and quantified in surface water from the Netherlands. H-PFCA concentrations are comparable among the sampling sites, suggesting that their presence in Dutch surface water is less likely to be from a point source (e.g. a manufacturing plant) but more from environmental transport from other sources. This potentially reinforces the hypothesis by Song et al. (2018), that efficient transport could lead to the global distribution of emerging C_3–C_9 PFASs in surface water. As opposed to findings reported by Liu et al. (2015), and Song et al. (2018), no H–PFCAs with chain-length C6, C8, C9, and C10 were detected, possibly due to the lower transport efficiency of these longer-chain H–PFCAs. In addition, we hypothesize that the absence of 4H-PFBA and 5H-PFPA in the study from Liu et al., and Song et al. may be due to insufficient chromatography for the short-chained H–PFCAs. For example, $C_6F_{10}HO_2^-$ was reported to be eluting around 4.12 min with a rather broad peak-shape and including a shoulder by Liu et al. (2015). Using TBAS as an ion-pairing agent could potentially reveal additional alternatives in these samples.

4. Conclusion

4.1. (H-)PFCA method development, validation, and application

A UHPLC-MS/MS method for the simultaneous detection and quantification of PFCAs and H–PFCAs in water was developed and validated. The use of the ion-pairing agent TBAS improved peak shape and retention for short-chained (H-)PFCAs. For eleven of the 14 PFASs included in this study (i.e. PFHxA, PFHpA, 7H-PFHpA, PFOA, 8H-PFOA, PFNA, 9H-PFNA, PFDA, PFUnDA, 11H-PFUnDA, PFDoDA), linearity, matrix effects, absolute recovery, trueness, repeatability, and within-lab reproducibility were deemed acceptable.

Table 4
Concentrations of detectable PFCAs and H–PFCAs (in ng/L) in surface water from the Netherlands.

Sampling location[a]	PFPA	PFHxA	PFHpA	PFOA	PFNA	PFDA	PFUnDA	∑ PFCAs	4H-PFBA	5H-PFPA	7H-PFHpA	∑ H–PFCAs
R1	21.9	9.6	4.6	12.6	1.2	1.3	0.1	51.3	1.6	0.6	<LOD[d]	2.2
R2	89.5	11.1	5.3	14.1	0.8	0.8	<LOD[d]	121.6	1.6	0.6	<LOD[d]	2.2
R3	5.1	12.8	5.2	25.1	0.9	1.5	0.3	50.9	1.8	<LOD[d]	<LOD[d]	1.8
R4	>125[b]	11.1	5.5	13.2	1.5	3.8	0.5	35.6	1.4	<LOD[d]	<LOD[d]	1.4
R5	11.1	10.8	4.3	13.8	0.9	1.3	0.2	42.4	1.9	<LOD[d]	<LOD[d]	1.9
R6	11.9	14.1	9.5	>125[b]	1.2	1.5	0.1	38.3	1.4	<LOD[d]	0.3[c]	1.7
R7	7.6	8.3	4.4	10.3	1.1	0.8	<0.1[c]	32.5	1.7	0.6	<LOD[d]	2.3
R8	8.8	7.5	3.3	8.4	0.9	0.9	0.1	29.9	1.7	<LOD[d]	<LOD[d]	1.7
R9	>125[b]	16.0	5.2	10.3	1.1	1.8	0.1	34.5	1.7	<LOD[d]	<LOD[d]	1.7
R10	11.0	10.4	4.2	13.1	1.1	0.8	0.2	40.8	2.0	<LOD[d]	<LOD[d]	2
R11	77.4	12.5	4.0	10.6	0.7	0.7	<LOD[d]	105.9	1.9	0.6	<LOD[d]	2.5

[a] See Fig. 1 for the exact sampling location.
[b] Above dynamic range calibration curve.
[c] Detected and below LOD, see Table 2 for LODs for individual PFCAs and H–PFCAs.
[d] Below LOD, see Table 2 for LODs for individual PFCAs and H–PFCAs.

The validated method was applied to surface water samples collected in the Netherlands, whereby ∑H-PFCA concentrations were generally comparable at all sampling locations and 27 times lower compared to ∑PFCA concentrations. This study reports for the first time the detection of H–PFCAs in surface water from the Netherlands. These results emphasize the need for validated analytical methods for emerging PFASs currently being detected in increasing numbers in the environment.

Credit author statement

Mo Awchi: Conceptualization, Methodology, Formal analysis, Investigation, Writing – original draft, Visualization. Wouter A. Gebbink: Conceptualization, Methodology, Writing – review & editing, Supervision, Visualization. Bjorn JA Berendsen: Writing – review & editing, Supervision. Jonathan P. Benskin: Writing – review & editing, Supervision. Stefan PJ van Leeuwen: Conceptualization, Methodology, Resources, Writing – review & editing, Visualization, Supervision, Funding acquisition.

Declaration of competing interest

The authors declare that they have no known competing financial interests or personal relationships that could have appeared to influence the work reported in this paper.

Acknowledgements

We gratefully acknowledge our colleagues Liz Leenders, Thijs Hensema, Anand Gavai, Ed Boers, Robin Wegh, Arjen Gerssen, and Arjen Lommen for their inspiring discussions supporting this project.

Appendix A. Supplementary data

Supplementary data to this article can be found online at https://doi.org/10.1016/j.chemosphere.2021.132143.

References

Barrett, H., Du, X., Houde, M., Lair, S., Verreault, J., Peng, H., 2021. Suspect and nontarget screening revealed class-specific temporal trends (2000–2017) of poly-and perfluoroalkyl substances in st. Lawrence Beluga whales. Environ. Sci. Technol. 1659–1671.

Berendsen, B., Lakraoui, F., Leenders, L., Van Leeuwen, S., 2020. The analysis of perfluoroalkyl substances at ppt level in milk and egg using UHPLC-MS/MS. Food Addit. Contam. 1707–1718.

Buck, R.C., Franklin, J., Berger, U., Conder, J.M., Cousins, I.T., de Voogt, P., Jensen, A.A., Kannan, K., Mabury, S.A., van Leeuwen, S.P., 2011. Perfluoroalkyl and polyfluoroalkyl substances in the environment: terminology, classification, and origins. Integrated Environ. Assess. Manag. 513–541.

DeWitt, J.C., 2015. Toxicological Effects of Perfluoroalkyl and Polyfluoroalkyl Substances. Springer.

EFSA, Schrenk, D., Bignami, M., Bodin, L., Chipman, J.K., del Mazo, J., Grasl-Kraupp, B., Hogstrand, C., Hoogenboom, L., Leblanc, J.C., 2020. Risk to human health related to the presence of perfluoroalkyl substances in food. EFSA Journal 18, e06223.

EPA, E.P.A., 2000. EPA and 3M ANNOUNCE PHASE OUT of PFOS.

Esparza, X., Moyano, E., De Boer, J., Galceran, M., Van Leeuwen, S., 2011. Analysis of perfluorinated phosponic acids and perfluorooctane sulfonic acid in water, sludge and sediment by LC–MS/MS. Talanta 86, 329–336.

EU, E.C., 2002. 2002/657/EC: commission Decision of 12 August 2002 implementing Council Directive 96/23/EC concerning the performance of analytical methods and the interpretation of results. Official Journal of the European Communities.

EURL, P., 2019. Nº SANTE/12682/2019.

Fromme, H., Wöckner, M., Roscher, E., Völkel, W., 2017. ADONA and perfluoroalkylated substances in plasma samples of German blood donors living in South Germany. Int. J. Hyg Environ. Health 455–460.

Gaballah, S., Swank, A., Sobus, J.R., Howey, X.M., Schmid, J., Catron, T., McCord, J., Hines, E., Strynar, M., Tal, T., 2020. Evaluation of developmental toxicity, developmental neurotoxicity, and tissue dose in zebrafish exposed to GenX and other PFAS. Environ. Health Perspect., 047005

Gebbink, W.A., Van Asseldonk, L., Van Leeuwen, S.P., 2017. Presence of emerging per- and polyfluoroalkyl substances (PFASs) in river and drinking water near a fluorochemical production plant in The Netherlands. Environ. Sci. Technol. 11057–11065.

Glüge, J., Scheringer, M., Cousins, I.T., DeWitt, J.C., Goldenman, G., Herzke, D., Lohmann, R., Ng, C.A., Trier, X., Wang, Z., 2020. An overview of the uses of per-and polyfluoroalkyl substances (PFAS). Environ. Sci. Processes Impacts 2345–2373.

Hensema, T.J., Berendsen, B.J., van Leeuwen, S.P., 2021. Non-targeted identification of per-and polyfluoroalkyl substances at trace level in surface water using fragment ion flagging. Chemosphere 265, 128599.

Krippner, J., Falk, S., Brunn, H., Georgii, S., Schubert, S., Stahl, T., 2015. Accumulation potentials of perfluoroalkyl carboxylic acids (PFCAs) and perfluoroalkyl sulfonic acids (PFSAs) in maize (Zea mays). J. Agric. Food Chem. 3646–3653.

Li, F., Duan, J., Tian, S., Ji, H., Zhu, Y., Wei, Z., Zhao, D., 2020a. Short-chain per-and polyfluoroalkyl substances in aquatic systems: occurrence, impacts and treatment. Chem. Eng. J. 122506.

Li, Y., Yu, N., Du, L., Shi, W., Yu, H., Song, M., Wei, S., 2020b. Transplacental transfer of per-and polyfluoroalkyl substances identified in paired maternal and cord sera using suspect and nontarget screening. Environ. Sci. Technol. 3407–3416.

Liu, Y., Pereira, A.D.S., Martin, J.W., 2015. Discovery of C5–C17 poly-and perfluoroalkyl substances in water by in-line SPE-HPLC-Orbitrap with in-source fragmentation flagging. Anal. Chem. 87, 4260–4268.

Liu, J., Li, C., Qu, R., Wang, L., Feng, J., Wang, Z., 2018. Kinetics and mechanism insights into the photodegradation of hydroperfluorocarboxylic acids in aqueous solution. Chem. Eng. J. 644–652.

Newton, S., McMahen, R., Stoeckel, J.A., Chislock, M., Lindstrom, A., Strynar, M., 2017. Novel polyfluorinated compounds identified using high resolution mass spectrometry downstream of manufacturing facilities near Decatur, Alabama. Environ. Sci. Technol. 1544–1552.

CAS No: 335-67-1, PFOA, perfluorooctanoic acid), its salts and PFOA-related compounds in annexes A, B and/or C to the Stockholm convention on persistent organic pollutants.

OECD, 2021. Comprehensive Global Database of PFASs.

P.O.P.R., C.P.O.P.R., 2015. Persistent organic pollutants review committee proposal to list pentadecafluorooctanoic acid.

Sheng, N., Cui, R., Wang, J., Guo, Y., Wang, J., Dai, J., 2018. Cytotoxicity of novel fluorinated alternatives to long-chain perfluoroalkyl substances to human liver cell line and their binding capacity to human liver fatty acid binding protein. Arch. Toxicol. 359–369.

Song, X., Vestergren, R., Shi, Y., Huang, J., Cai, Y., 2018. Emissions, transport, and fate of emerging per-and polyfluoroalkyl substances from one of the major fluoropolymer manufacturing facilities in China. Environ. Sci. Technol. 9694–9703.

Swedish Chemicals Agency, K., 2021. Per- and polyfluoroalkyl substances (PFAS). https://www.kemi.se/en/chemical-substances-and-materials/highly-fluorinated-substances.

Wang, Y., Yu, N., Zhu, X., Guo, H., Jiang, J., Wang, X., Shi, W., Wu, J., Yu, H., Wei, S., 2018. Suspect and nontarget screening of per-and polyfluoroalkyl substances in wastewater from a fluorochemical manufacturing park. Environ. Sci. Technol. 11007–11016.

Washington, J.W., Jenkins, T.M., Weber, E.J., 2015. Identification of unsaturated and 2H polyfluorocarboxylate homologous series and their detection in environmental samples and as polymer degradation products. Environ. Sci. Technol. 13256–13263.

Xiao, F., 2017. Emerging poly-and perfluoroalkyl substances in the aquatic environment: a review of current literature. Water Res. 482–495.

Zhang, C., Hopkins, Z.R., McCord, J., Strynar, M.J., Knappe, D.R., 2019. Fate of per-and polyfluoroalkyl ether acids in the total oxidizable precursor assay and implications for the analysis of impacted water. Environ. Sci. Technol. Lett. 662–668.